

# FATIGUE AND FRACTURE BEHAVIOR OF HIGH TEMPERATURE MATERIALS

*Edited by: Peter K. Liaw*

## Mechanisms of High-Temperature Fatigue in Silicon Carbide Ceramics

*D. Chen, X.F. Zhang, and R.O. Ritchie*

Pgs. 1-8

# TMS

184 Thorn Hill Road  
Warrendale, PA 15086-7514  
(724) 776-9000

# MECHANISMS OF HIGH-TEMPERATURE FATIGUE AND FRACTURE IN SILICON CARBIDE CERAMICS

Da Chen, Xiao-Feng Zhang, and Robert O. Ritchie

Materials Sciences Division, Lawrence Berkeley National Laboratory, and  
Department of Materials Science and Engineering,  
University of California, Berkeley, CA 94720

## Abstract

The high-temperature mechanical properties of an *in situ* toughened silicon carbide, with Al, B and C sintering additives (ABC-SiC), have been examined at temperatures from ambient to 1300°C with the objective of characterizing the role of the grain-boundary phase. It was found that elevated temperatures up to 1300°C do not severely compromise the strength, toughness and fatigue resistance of ABC-SiC, compared to properties at ambient temperatures. Mechanistically, the damage and shielding mechanisms governing cyclic fatigue-crack advance are essentially unchanged between ~25° and 1300°C, involving a mutual competition between intergranular cracking ahead of the crack tip and interlocking grain bridging in the crack wake. The unusually good high-temperature properties of ABC-SiC are attributed to *in situ* crystallization of grain-boundary amorphous phase, which on subsequent cooling also marginally enhances the ambient-temperature mechanical properties. In comparison to commercial SiC (Hexoloy), the ABC-SiC displays superior strength, fracture toughness, and fatigue-crack growth resistance at all temperatures from 25° to 1300°C.

## Introduction

As a high-temperature structural material, silicon carbide (SiC) ceramics offer many advantages, including a high melting temperature, low density, high elastic modulus and strength, and good resistance to creep, oxidation and wear. This combination of properties makes it a promising candidate for use in such applications as gas turbines, piston engines and heat exchangers (1,2), although its use to date has been severely limited by its poor toughness properties.

The low inherent fracture toughness of conventional SiC ceramics ( $K_{Ic}$  is typically ~2-3 MPa√m) can be improved, however, by several processing and reinforcement routes. One approach is to

produce a composite, which is typically accomplished by incorporating continuous fibers, whiskers, platelets, or second phase particles (3). For monolithic ceramics, *in situ* toughening can also be effective with microstructures consisting of elongated grains encased with a residual glassy film. Such microstructures induce intergranular fracture and are thus effective in promoting toughening from the consequent crack bridging, as has been well demonstrated in silicon nitride (Si<sub>3</sub>N<sub>4</sub>) ceramics (4). The problem in monolithic ceramics is that although the amorphous grain-boundary film is critical for good low-temperature toughness, its presence at high temperatures provides a preferred site for softening and creep cavitation, which typically limits the high-temperature strength, creep and oxidation resistance.

Recently, in an attempt to avoid such tradeoffs between low-temperature toughness and high-temperature strength, a monolithic SiC with additions of Al metal as well as B and C (termed ABC-SiC) has been developed. At ambient temperatures, ABC-SiC exhibits fracture toughnesses as high as 9 MPa√m with strengths of ~650 MPa (5), mechanical properties that are among the highest reported for SiC. The high toughness has been attributed to various crack-bridging processes in crack wake resulting from the intergranular crack path (6); specifically, crack-tip shielding from both elastic bridging and frictional pullout of the grains provide the major contributions, with the frictional pullout component being the more potent. At elevated temperatures, however, a critical factor governing properties is the viscosity of the grain-boundary phase, which results from the presence of sintering additives that are present as densification aids (7). The softening of this phase can severely degrade properties (8); however, *in situ* crystallization can provide an excellent means to increase its viscosity at such high temperatures.

In the present work, we examine how the elevated temperature mechanical properties of ABC-SiC are affected by the nature of the grain-boundary film/phase, and investigate whether its superior room-temperature strength and fracture toughness

properties (5,6) can be retained at high temperatures. In addition, we specifically investigate the high-temperature cyclic fatigue properties, in part due to the contradictory nature (9-17) and paucity of published results on this topic to date.

### Experimental Procedures

#### Material processing

ABC-SiC was processed with submicron  $\beta$ -SiC starting powders, which were mixed with additions of 3 wt.% Al powder (nominal particle diameter  $\sim 5 \mu\text{m}$ ), 0.6 wt.% B powder, and 2 wt.% C (as Apiezon wax). The Apiezon wax, which also served as a binder, was dissolved in toluene, and the other powders added; the resulting suspension was agitated ultrasonically for 5-10 min to minimize agglomerate formation, and then stir-dried. The dried material was then ground in a mortar and pestle prior to sieving through a 200 mesh screen.

Hot-pressing was conducted for 1 h at  $1900^\circ\text{C}$ , at 50 MPa pressure in a flowing argon atmosphere, in a graphite die using green compacts that were previously formed by uniaxial compression at 35 MPa in a metal die. The resulting hot-pressed disks were surface-ground, and polished to a  $1 \mu\text{m}$  diamond powder finish, prior to the machining of samples.

#### High-temperature mechanical properties tests

Fracture toughness ( $K_{IC}$ ) and cyclic fatigue-crack growth tests were performed on disk-shaped compact-tension DC(T) specimens (28 mm wide, 3 mm thick), containing "large" ( $> 3 \text{ mm}$ ) through-thickness cracks. Toughness testing was performed on fatigue pre-cracked specimens at temperatures between 25 and  $1300^\circ\text{C}$ ; in addition, the toughness of as-processed samples was compared with those following a prior thermal exposure for 85 hr at  $1300^\circ\text{C}$ . Strength tests were performed in four-point bend on  $3 \text{ mm} \times 3 \text{ mm} \times 30 \text{ mm}$  beam specimens.

Cyclic fatigue-crack growth testing was performed in general accordance with ASTM Standard E-647. Specifically, DC(T) specimens were cycled at 550, 850, 1200 and  $1300^\circ\text{C}$  under automated stress-intensity stress intensity ( $K$ ) control while maintaining a constant load ratio (ratio of minimum to maximum applied loads) of  $R = 0.1$  at frequencies of  $\nu = 3$  and 25 Hz (sinusoidal waveform); corresponding tests at  $25^\circ\text{C}$  were carried out under the same conditions only at frequencies of 25 and 1000 Hz.

All toughness and crack growth experiments were conducted on computer-controlled servo-hydraulic mechanical testing machines. Elevated temperature tests were performed in an environmental chamber/furnace with graphite elements that maintain temperature to within  $\pm 1^\circ\text{C}$ . The test environment at elevated temperatures was flowing gaseous argon at atmospheric pressure; corresponding tests at  $25^\circ\text{C}$  were conducted in room air. Crack lengths were continuously monitored *in situ* at elevated temperatures by a direct-current electrical-potential drop technique (18,19).

#### Microstructural characterization

All fracture surfaces and crack profiles were imaged in a field-emission scanning electron microscope (FESEM). The atomic and structural nature of the grain boundaries was also examined using high-resolution transmission electron microscopy (HRTEM)

Chemical compositions of any grain-boundary phases were analyzed using X-ray energy-dispersive spectrometer (XEDS) with a 8 nm probe. In addition, the microstructure and damage in regions directly ahead of the crack tip were examined in the transmission electron microscope (TEM). Specifically, 3-mm diameter TEM foils were taken from the crack-tip region of fracture and fatigue test specimens such that the crack line was parallel to the axis of the foil with the crack tip located  $\sim 500 \mu\text{m}$  away from the foil center. The foils, which were ground down to  $20 \mu\text{m}$  using a precision dimpling machine and further thinned by argon ion milling, were examined on a Philips CM200 microscope, operating at 200 kV.

### Results and Discussion

#### As-processed microstructure

The microstructure of as-processed ABC-SiC consisted of a network of interlocking plate-like grains of 5 vol.%  $\beta$ -phase (cubic polytype 3C) and 95 vol.%  $\alpha$ -phase (49 vol.% 4H and 46 vol.% 6H hexagonal polytypes), with a maximum grain aspect ratio of  $\sim 4$  to 5. Between the grains, an amorphous grain-boundary film, typically  $\sim 1 \text{ nm}$  thick and rich in Al, O and C (20), can be seen in the hot-pressed material (Fig. 1). The remaining sintering additives were found to form bulk secondary phases at triple-junctions and multigrain-junctions (5,21). In addition, in specific  $\alpha$ -SiC grains, the presence of isolated dislocations could be seen; these dislocations, which were always in very low densities, are likely to be partial dislocations bounding the stacking faults.

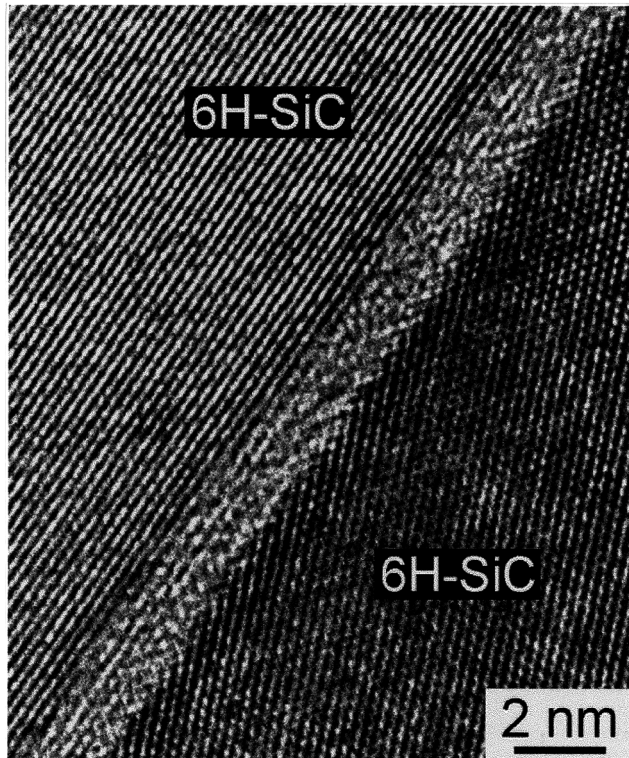


Figure 1: High-resolution transmission electron micrograph of as-processed ABC-SiC, showing the amorphous grain-boundary film.

### Strength and fracture toughness

Table I Fracture toughness and strength in as-processed (amorphous grain boundaries) and 1300°C pre-exposed (crystallized grain boundaries) ABC-SiC tested at 25 and 1300°C. The corresponding data for commercial SiC (Hexoloy) are also listed for comparison.

	Fracture toughness (MPa√m)		Strength (MPa)
	25°C	1300°C	25°C
as-processed	6.2	4.3	620
pre-exposed	7.2	5.2	604
SiC (Hexoloy)	2.5	1.9	380

The fracture toughness of the as-processed ABC-SiC was measured as  $K_c = 6.2 \text{ MPa}\sqrt{\text{m}}$  at 25°C and  $4.3 \text{ MPa}\sqrt{\text{m}}$  at 1300°C. However, annealing for 85 h at 1300°C led to a ~20% increase in these values (Table I). Moreover, such thermal annealing can also increase the high-temperature strength; specifically, annealing for 7 days at 1500°C led to a four-fold increase in the bend strength in this ceramic at 1300°C (22). It should be noted that the corresponding strength and toughness properties of commercial SiC (Hexoloy) are a factor of ~2 to 3 times lower.

Following such prolonged high-temperature annealing, HRTEM imaging indicated that a large majority of the grain-boundary glassy films had become fully crystallized in both toughness and strength testing specimens (Fig. 2); this was found to occur at all temperatures above ~1100°C for times in excess of ~5 h. Moreover, the average thickness of grain-boundary film decreased to less than ~1 nm, with a corresponding increase in the Al concentration revealed by the XEDS spectra (20). Such crystallization of the grain-boundary phase clearly would minimize softening and grain-boundary sliding and possibly induced flaw healing within this region, which would account for the four-fold increase in strength.

In contrast, although such crystallization is less common in  $\text{Si}_3\text{N}_4$ , when it does occur it has been found to *degrade* the subsequent low temperature strength and toughness (23). Remarkably, in ABC-SiC, after crystallization the strength at 25°C was increased by ~16%, and the toughness increased by some 16 to 21% at both 25 and 1300°C (Table I). Since microstructural changes often have opposing effects in ceramics, e.g., coarsening grain sizes in  $\text{Al}_2\text{O}_3$  and  $\text{Si}_3\text{N}_4$  SiC can promote toughness yet decrease strength, the process of *in situ* (or thermally-induced) crystallization of the grain-boundary phase in ABC-SiC is particularly effective as it acts to increase both strength and toughness, with only a small reduction in properties at elevated temperatures (up to 1300°C).

It is uncertain why the crystallization of the grain-boundary films should lead to a slight improvement in the subsequent toughness and fatigue resistance at room temperature. However, as stated above, the mechanisms of both fracture and fatigue are associated with grain bridging, resulting from the frictional tractions generated via contact of opposing crack faces (24). The pullout resistance, represented by bridging stress, acts to reduce the near-tip crack-driving force for crack extension; its magnitude is linearly proportional to the frictional coefficient between sliding grain faces (25). Crystallization of the grain-boundary phase is expected to increase the frictional coefficient, and the resulting

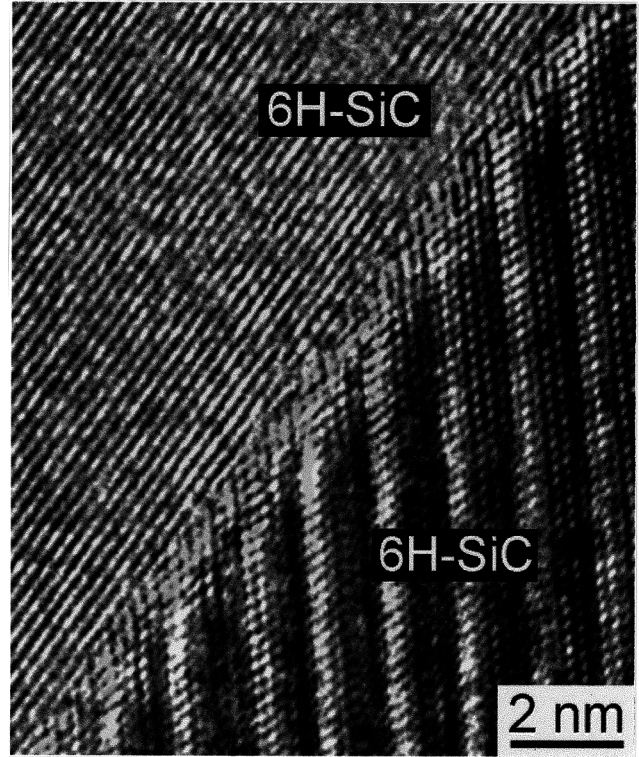


Figure 2: High-resolution transmission electron micrograph of a grain boundary in ABC-SiC after high-temperature annealing (1400°C/840h), showing that amorphous layer has become fully crystallized.

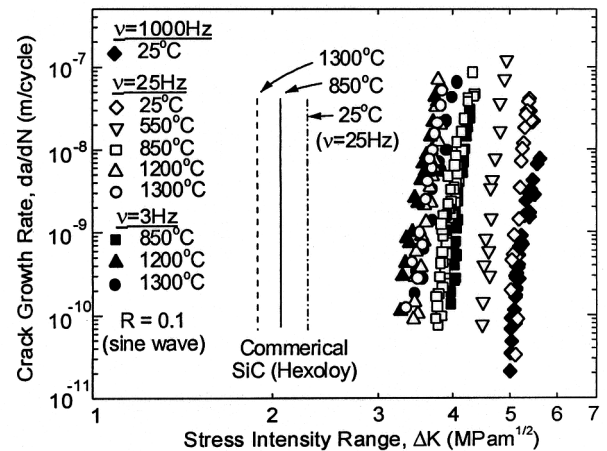


Figure 3: Cyclic fatigue-crack growth rates,  $da/dN$ , in ABC-SiC as a function of the applied stress-intensity range  $\Delta K$  for the tests conducted at temperatures between 25 and 1300°C, load ratio  $R = 0.1$ , and frequencies between 3 and 1000 Hz. For comparison, the crack growth behavior of commercial SiC (Hexoloy) were also illustrated.

increase in the bridging stress may well provide the origin of the enhanced grain bridging.

### Fatigue-crack growth behavior

Fig. 3 illustrates the variation in fatigue-crack growth rates,  $da/dN$ , with applied stress-intensity range,  $\Delta K$ , for ABC-SiC at a load ratio of 0.1; shown are the effects of temperature and loading frequency. It can be seen that at both ambient and elevated temperatures, crack-growth rates display a marked sensitivity to the stress intensity regardless the loading frequency; this is a common characteristic of monolithic ceramics at low homologous temperatures (26). In terms of a simple Paris power-law formation:

$$da/dN = C \Delta K^m, \quad (1)$$

(where  $C$  and  $m$  are scaling constants), these data show a Paris exponent  $m$  between 35 and 68.

Although changing the cyclic frequency over the range 3 to 1000 Hz has little effect on fatigue-crack growth behavior, growth rates are accelerated with increasing temperature. Indeed,  $\Delta K_{th}$  fatigue thresholds decrease from just over 5 MPa $\sqrt{m}$  at 25°C to between 3.3 and 3.4 MPa $\sqrt{m}$  at 1200°C; interestingly, there is no further decline at 1300°C. Mechanistically, the lack of a frequency effect in ABC-SiC at ambient temperatures is expected as crack advance occurs via predominantly intergranular cracking ahead of the tip, balanced by shielding by grain bridging in the wake, both essentially rate-insensitive processes (27-29). However, the absence of a frequency effect at elevated temperatures is much more surprising, particularly since comparable materials, such as Si<sub>3</sub>N<sub>4</sub>, Al<sub>2</sub>O<sub>3</sub> and silicide-matrix ceramics, show a marked sensitivity to frequency at temperatures due to the onset of creep damage above ~1000°C (9,12-14,30). As described below, fatigue fracture mechanisms at 850 to 1300°C in the present material are effectively identical to those at room temperature, which is consistent with the absence of significant creep phenomena at, and below, 1300°C.

Similar to the toughness properties, the fatigue-crack growth resistance of ABC-SiC was also found to be far superior to commercial SiC (Hexoloy) at both room and elevated temperatures. Results at 25 to 1300°C, which are compared to ABC-SiC in Fig. 3, indicate that Hexoloy fails catastrophically, with no cycle-dependent cracking, at stress intensities some 40-50% lower than the fatigue thresholds in ABC-SiC. Such extremely brittle behavior is attributed to the absence of toughening from crack bridging behind the crack tip, resulting from its fully transgranular mode of fracture (Hexoloy shows little to no evidence of an amorphous grain-boundary film).

A comparison of the crack-growth velocities under cyclic and static (sustained) loading is shown in Fig. 4. It can be seen that at both ambient and elevated temperatures, growth rates in ABC-SiC are significantly faster under cyclic loads than under sustained loading (static fatigue) at equivalent stress-intensity levels. Such behavior has been observed previously in Mg-PSZ (31,32), Al<sub>2</sub>O<sub>3</sub> (33) and Si<sub>3</sub>N<sub>4</sub> (34), and is consistent with the fact that at low temperatures, crack-advance (damage) mechanisms are identical under both types of loading; specifically, it is the cyclic-loading induced degradation in wake shielding that accelerates growth rates under cyclic loads. In contrast, the sustained-load mechanisms at elevated temperatures are generally far more damaging in such ceramics as Al<sub>2</sub>O<sub>3</sub> and Si<sub>3</sub>N<sub>4</sub> (9,13-15) because of the onset of creep damage, which can cause softening and

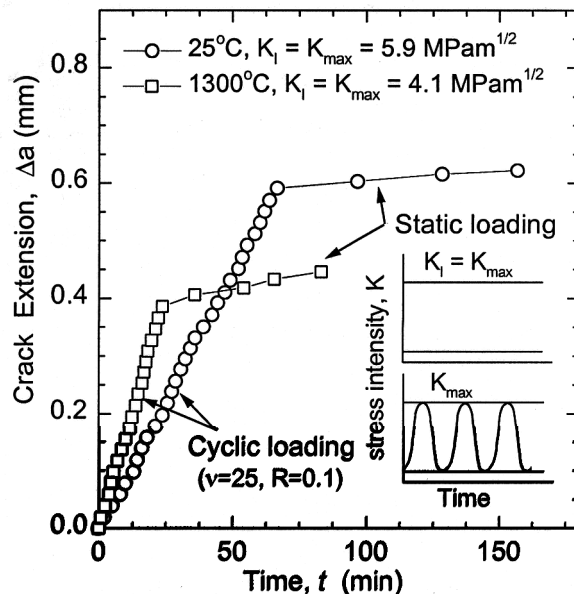


Figure 4: Crack extension,  $\Delta a$ , plotted as function of time,  $t$ , demonstrating the effect of sustained loading vs. cyclic loading conditions, at a fixed maximum stress intensity ( $K_I = K_{max}$ ). Plotted is behavior at 25°C, where  $K_I = K_{max} = 5.9 \text{ MPa}\sqrt{m}$ , and at 1300°C, where  $K_I = K_{max} = 4.1 \text{ MPa}\sqrt{m}$ .

cavitation in the grain-boundary films (10). Such behavior was not seen in ABC-SiC at temperatures up to 1300°C.

Scanning electron microscopy (SEM) of fracture surfaces and crack profiles in ABC-SiC at 1300°C revealed a predominantly intergranular fracture under both static and cyclic loads (Fig. 5a,c), with extensive interlocking grain bridging behind the crack tip (Fig. 5b,d). Also noticeable on the cyclic fatigue surfaces was the presence of debris, formed by wear and abrasion of the bridging crack faces during cycling. Fracture surfaces at 25°C were essentially identical (6), implying that a similar sequence of mechanisms, namely intergranular cracking coupled with degradation of the resulting wake zone of bridging grains, is active at both temperatures.

TEM studies of regions in the immediate vicinity of the crack tip provided direct confirmation of these observations. Akin to behavior at room temperature, crack extension at 1300°C under both sustained and cyclic loading was predominantly along the grain boundaries with no indication of cavitation damage ahead of the tip or viscous-phase bridging in the wake (Fig. 6). HRTEM observations also revealed that the grain-boundary films had fully crystallized (e.g., Fig. 2) *in situ* during the high-temperature fatigue tests, which typically lasted ~3 to 10 days at 1200 or 1300°C.

The absence of creep damage and/or viscous softening of the grain-boundary phase at 1300°C in ABC-SiC is quite startling. In Si<sub>3</sub>N<sub>4</sub> (11,12), Al<sub>2</sub>O<sub>3</sub> (13) and silicide-matrix composites (30) at these temperatures, cavitation along grain boundaries, microcracking zones, and viscous-phase bridging are commonly observed. It is apparent that the unique high-temperature characteristics of ABC-SiC appear to be a result of the *in situ* crystallization of grain-boundary glassy phase.

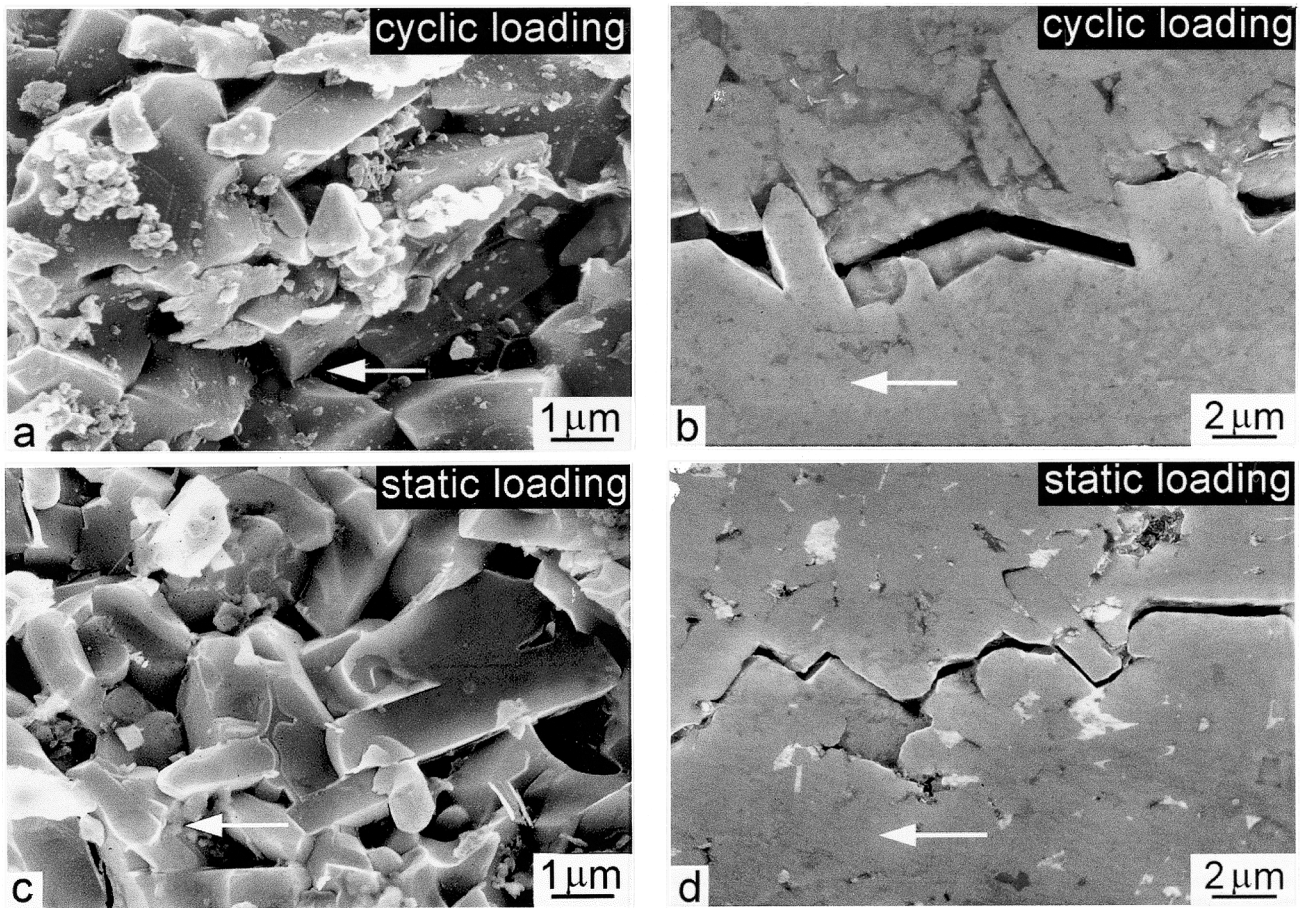


Figure 5: Scanning electron micrographs of (a,c) fracture surfaces and (b,d) crack trajectories behind the crack tip in ABC-SiC at 1300°C under (a,b) cyclic loading with frequency  $\nu = 25$  Hz, load ratio  $R = 0.1$  and maximum stress intensity  $K_{\max} = 4.1$  MPa $\sqrt{m}$ ; and (c,d) static loading with stress intensity factor  $K_I = 4.1$  MPa $\sqrt{m}$ . Arrows indicate direction of crack propagation.

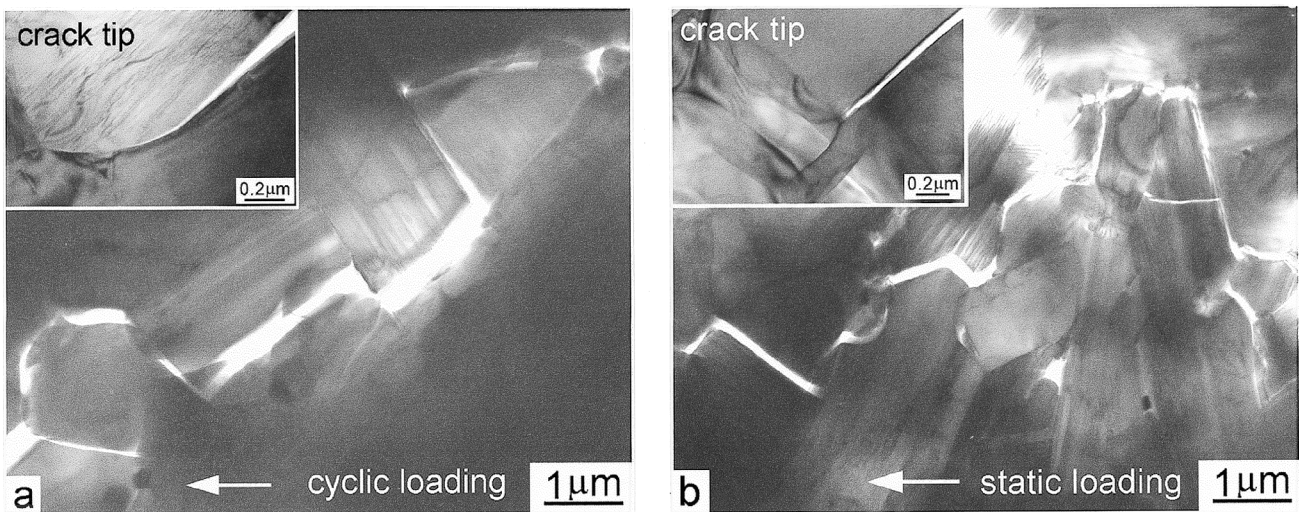


Figure 6: Transmission electron micrographs of the crack profiles at the crack tip region in ABC-SiC at 1300°C under (a) cyclic loading ( $R = 0.1$ ,  $\nu = 25$  Hz,  $K_{\max} = 4.1$  MPa $\sqrt{m}$ ); and (b) sustained loading ( $K_I = 4.1$  MPa $\sqrt{m}$ ). Arrows indicate the general direction of crack propagation.

Even though the primary mechanisms of damage (intergranular cracking) and shielding (grain bridging) are apparently unchanged between 25 and 1300°C in ABC-SiC, there is a small change in the fatigue-crack growth resistance in that fatigue thresholds  $\Delta K_{th}$  are approximately 30% lower at the higher temperature. This may be rationalized by considering the nature of grain bridging (35) and its degradation under cyclic loading due to frictional wear (36,37). The pullout resistance from frictional tractions generated via sliding contact of opposing crack faces (38) is proportional to the normal stress acting on the interface, which in turn is a function of the residual stress resulting from thermal expansion anisotropy during cooling from the processing temperature. As the residual stresses will “anneal out” with increasing temperature, the normal stress will decrease. However, once crystallization of the grain-boundary phase occurs above ~1100°C, as stated above, the frictional coefficient may be expected to be higher. Thus, the minimal change in cyclic fatigue properties between 25 and 1300°C can be related to (i) the lack of any apparent change in mechanisms, (ii) the fact that the decrease in residual stress with temperature is compensated by an increase in the frictional coefficient, and (iii) the absence of significant creep damage, the latter two effects being associated with the *in situ* crystallization of the grain-boundary phase. Such a result is consistent with previous studies in other ceramics that show a beneficial effect of crystallization on oxidation and mechanical properties at elevated temperatures (39-41).

The beneficial effect of the crystallization of glassy phase is also clearly demonstrated by the creep behavior. Following an initial primary creep stage with primary strain  $\epsilon_p \approx 0.001$ , steady-state creep rates,  $\dot{\epsilon}$ , in ABC-SiC are relatively low, i.e.,  $\dot{\epsilon} < 2 \times 10^{-10}$  /s at 1200°C and  $\dot{\epsilon} = 6 \times 10^{-10}$  /s at 1300°C under the load of  $\sigma = 100$  MPa (22). In comparison, Hexoloy exhibits far higher creep rates, i.e.,  $\epsilon_p \approx 0.018$  and  $\dot{\epsilon} \approx 8.8 \times 10^{-9}$  /s at 1200°C ( $\sigma = 139$  MPa) (22). Similarly, in Si<sub>3</sub>N<sub>4</sub>-GN-10, creep rates are an order of magnitude faster, i.e.,  $\epsilon_p \approx 0.009$ ,  $\dot{\epsilon} = 1.78 \times 10^{-9}$  /s at 1300°C ( $\sigma = 100$  MPa) (42). ABC-SiC also exhibited low creep rates at stresses that were a much higher percentage of its fracture strength than the silicon nitrides; for example, the Si<sub>3</sub>N<sub>4</sub>/SiC nano-composite had a similar creep rate in bending at 1400°C, but with a bend strength 895 MPa (43), compared to ~300 MPa for ABC-SiC.

#### Concluding Remarks

Structural ceramics have often been regarded as exhibiting a conflict between toughness, strength, and fatigue resistance. Indeed, this conflict is not unlike the competition between brittleness and strength in metallic systems. A summary of many results on creep and toughness at 1300°C for SiC and Si<sub>3</sub>N<sub>4</sub>, extracted from the literature, is shown in Fig. 7, to illustrate this paradigm, and to show that ABC-SiC can be processed to negate it. Essential in the success of retaining simultaneously strength, toughness, fatigue and creep resistance, is the creation of a crystalline grain-boundary film that retains a stable structure and composition up to high temperatures. In ABC-SiC, this can be achieved *in situ* at elevated temperatures, or by a high temperature annealing process. Where high temperature post-processing treatments of this kind are relatively uncommon for enhancing the properties of ceramics, their value is evident here. It should be added that the beneficial effects of the Al, B, and C additives and the subsequent heat treatments could, at this time, not have been predicted from either first principle computations or existing lore, but rather resulted from extensive experimentation and application

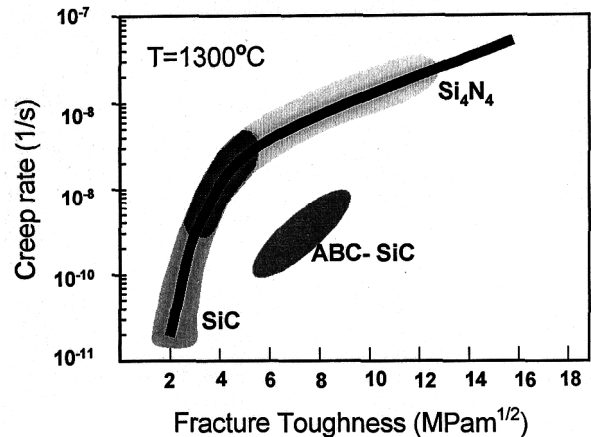


Figure 7: Summary of literature data on simultaneous creep and toughness values for SiC and Si<sub>3</sub>N<sub>4</sub> at 1300 °C. ABC-SiC can be processed to be significantly better than the general trend (courtesy of L. C. De Jonghe).

of general materials science principles. It is hoped that, in the future, computational efforts may assist in further developing the necessary nature and role of the grain-boundary films, to improve further the mechanical behavior of these high temperature structural ceramics.

#### Conclusions

The high-temperature mechanical properties, including strength, fracture toughness and cyclic fatigue properties, of an *in situ* toughened silicon carbide sintered with Al, B and C (ABC-SiC) have been studied, and related to the corresponding microstructural and mechanistic characteristics. Based on this work, the following conclusions can be made:

- (1) High-temperature annealing at 1100°C and above was found to lead to a remarkable improvement in strength and toughness properties. For example, the ~30% decrease in fracture toughness between 25 to 1300°C was partially offset by prior annealing for 85 h at 1300°C, which produced a ~20% increase of toughness at both 25 and 1300°C. Such annealing treatments were found to result in full crystallization of the glassy grain-boundary phase.
- (2) Cyclic fatigue-crack growth rates in ABC-SiC were only minimally increased, and  $\Delta K_{th}$  thresholds decreased by ~30%, with increase in temperature from 25 to 1300°C; behavior, however, was independent of frequency. At equivalent stress-intensity levels, crack-growth velocities under cyclic loads were significantly faster than those under static loads at both 25 and 1300°C. The fatigue-crack growth resistance of ABC-SiC was found to be superior to that of commercial SiC (Hexoloy) at all temperatures tested.
- (3) Crack profile and fractographic studies showed a predominantly intergranular cracking mode at both low and high temperatures, with crack-tip shielding by grain bridging in the crack wake. Such bridging was degraded under cyclic loads, as evidenced by the extensive wear debris on fatigue fracture surfaces. No evidence of creep cavitation or any form of viscous-ligament bridging by the grain-boundary glassy phase was seen at all temperatures up to 1300°C. The mechanistic sequence of intergranular damage ahead of the crack tip, and the cyclic-

loading induced degradation of grain bridging behind the tip, was considered to be essentially unchanged between 25 and 1300°C.

(4) HRTEM observations revealed that the grain boundary film/phase in specimens which underwent high-temperature ( $\geq 1100^\circ\text{C}$ ) fatigue/creep tests or prior annealing treatments were all fully crystallized. Such crystallized grain boundaries are considered to be the primary reason for the impressive mechanical properties of ABC-SiC at elevated temperatures, involving simultaneous enhancements in high-temperature strength, toughness, fatigue and creep resistance.

Acknowledgements This work was supported by the Director, Office of Science, Office of Basic Energy Sciences, Materials Sciences Division of the U.S. Department of Energy under Contract No. DE-AC03-76SF00098. Particular thanks are due to M. Sixta and L. C. DeJonghe (who developed ABC-SiC) for help with the processing and for discussions on their parallel studies on high-temperature strength and creep in ABC-SiC, and to J. M. McNaney and C. J. Gilbert for their help with experimentation.

### References

1. H. E. Helms and P. J. Haley, "Emerging Ceramic Components for Automotive Gas Turbines," in Third International Symposium on Ceramic Materials and components for Engines, (ed. V. J. Tennery, 1988), 1347-1364.
2. N. S. Jacobson, "Corrosion of Silicon-Based Ceramics in Combustion Environments," J. Am. Ceram. Soc., 76 (1993), 3-28.
3. A. G. Evans, "Perspective on the Development of High-Toughness Ceramics," J. Am. Ceram. Soc., 73 (1990), 187-206.
4. P. F. Becher, "Microstructural Design of Toughened Ceramics," J. Am. Ceram. Soc., 74 (1991), 255-269.
5. J. J. Cao, W. J. MoberlyChan, L. C. De Jonghe, C. J. Gilbert, and R. O. Ritchie, "In Situ Toughened Silicon Carbide with Al-B-C Additions," J. Am. Ceram. Soc., 79 (1996), 461-469.
6. C. J. Gilbert, J. J. Cao, W. J. MoberlyChan, L. C. De Jonghe, and R. O. Ritchie, "Cyclic Fatigue and Resistance-Curve Behavior of an In Situ Toughened Silicon Carbide with Al-B-C Additions," Acta materialia, 44 (1996), 3199-3214.
7. M. K. Ferber and M. G. Jenkins, "Evaluation of the Strength and Creep Fatigue Behavior of Hot Isostatically Pressed Silicon Nitride," J. Am. Ceram. Soc., 75 (1992), 2453-2462.
8. R. F. Davis and C. H. Carter, Jr., "A Review of Creep in Silicon Nitride and Silicon Carbide," in Advanced Ceramics, (ed. S. Saito, 1988), 95-125.
9. T. Hansson, Y. Miyashita, and Y. Mutoh, "High Temperature Crack Growth in Silicon Nitride with Two Different Grain Sizes under Static and Cyclic Loads," in Fracture Mechanics of Ceramics, Vol. 12, (ed. R. C. Bradt *et al.*, Plenum Press, New York, 1996), 187-202.
10. C. -K. J. Lin and D. F. Socie, "Static and Cyclic Fatigue of Alumina at High Temperatures," J. Am. Ceram. Soc., 74 (1991), 1511-1518.
11. U. Ramamurty, T. Hansson and S. Suresh, "High-Temperature Crack Growth in Monolithic and SiC<sub>w</sub>-Reinforced Silicon Nitride under Static and Cyclic Loads," J. Am. Ceram. Soc., 7 (1994), 2985-2999.
12. Y. H. Zhang and L. Edwards, "Cyclic Fatigue Crack Growth Behavior of Silicon Nitride at 1400°C," Mater. Sci. Eng., A256 (1998), 144-151.
13. L. Ewart and S. Suresh, "Elevated-Temperature Crack Growth in Polycrystalline Alumina under Static and Cyclic Loads," J. Mater. Sci., 27 (1992), 5181-5191.
14. S. -Y. Liu, I-W. Chen, and T. -Y. Tien, "Fatigue Crack Growth of Silicon Nitride at 1400°C: A Novel Fatigue-Induced Crack-Tip Bridging Phenomenon," J. Am. Ceram. Soc., 77 (1994), 137-142.
15. C. -K. J. Lin, M. G. Jenkins, and M. K. Ferber, "Cyclic Fatigue of Hot Isostatically Pressed Silicon Nitride at Elevated Temperatures," J. Mater. Sci., 29 (1994), 3517-3526.
16. M. G. Jenkins, M. K. Ferber and C. -K. J. Lin, "Apparent Enhanced Fatigue Resistance under Cyclic Tensile Loading for a HIPed Silicon Nitride," J. Am. Ceram. Soc., 76 (1993), 788-792.
17. A. G. Evans, L. R. Russel, and D. W. Richerson, "Slow Crack Growth in Ceramic Materials at Elevated Temperatures," Metall. Trans., 6A (1975), 707-716.
18. D. Chen, C. J. Gilbert and R. O. Ritchie, "In Situ Measurement of Fatigue Crack Growth Rates in a Silicon Carbide Ceramic at Elevated Temperatures Using a DC Potential System," Journal of Testing and Evaluation, 28 (2000), 236-241.
19. D. Chen, C. J. Gilbert, X. F. Zhang and R. O. Ritchie, "High-Temperature Cyclic Fatigue-Crack Growth Behavior in an In Situ Toughened Silicon Carbide," Acta Materialia, 48 (2000), 659-674.
20. X. F. Zhang, M. E. Sixta, and L. C. De Jonghe, "The Evolution of Grain Boundaries in SiC," J. Am. Ceram. Soc., (2000), in review.
21. T. D. Mitchell, L.C. De Jonghe, W. J. MoberlyChan, and R. O. Ritchie, "Silicon Carbide Platelet/Silicon Carbide Composites," J. Am. Ceram. Soc., 78 (1995), 97-103.
22. M. E. Sixta, "High-temperature Strength and Creep of SiC Sintered with Al, B, and C," (Ph.D. thesis, Department of Materials Science and Mineral Engineering, University of California, Berkeley, 2000).
23. T. Nishimura, M. Mitomo, and H. Suematsu, "High Temperature Strength of Silicon Nitride Ceramics with Ytterbium Silicon Oxynitride," J. Mater. Res., 12 (1997), 203-209.
24. P. L. Swanson, C. J. Fairbanks, B. R. Lawn, Y.-W. Mai, and B. J. Hockey, "Crack-Interface Grain Bridging as a Fracture Resistance Mechanism in Ceramics: I. Experimental Study on Alumina," J. Am. Ceram. Soc., 70 (1987), 279-289.
25. R. M. L. Foote, Y.-W. Mai, and B. Cotterell, "Crack Growth Resistance Curves in Strain-Softening Materials," J. Mech. Phys. Solids, 34 (1986), 593-607.
26. R. O. Ritchie and R. H. Dauskardt, "Cyclic Fatigue Ceramics: A Fracture Mechanics Approach to Subcritical Crack Growth and Life Prediction," J. Ceram. Soc. Jpn., 99 (1991), 1047-1062.
27. F. Guiu, M. Li and M. Reece, "Role of Crack-Bridging Ligaments in the Cyclic Fatigue Behavior of Alumina," J. Am. Ceram. Soc., 75 (1992), 2976-2984.
28. H. Kishimoto, A. Ueno and S. Okawara, "Crack Propagation Behavior of Polycrystalline Alumina under Static and Cyclic Loads," J. Am. Ceram. Soc., 77 (1994), 1324-1328.
29. M. Li and F. Guiu, "Subcritical Fatigue Crack Growth in Alumina - II. Crack Bridging and Cyclic Fatigue Mechanism," Acta Met. Mater., 43 (1995), 1871-1884.
30. U. Ramamurty, A. S. Kim, and S. Suresh, "Micromechanisms of Creep-Fatigue Crack Growth in a Silicide-Matrix Composite with SiC Particle," J. Am. Ceram. Soc., 76 (1994), 1953-1964.
31. R. H. Dauskardt, W. Yu, and R. O. Ritchie, "Fatigue Crack Propagation in Transformation-Toughened Zirconia Ceramic," J. Am. Ceram. Soc., 70 (1987), C-248-252.

32. R. H. Dauskardt, D. B. Marshall, and R. O. Ritchie, "Cyclic Fatigue-Crack Propagation in Magnesia-Partially-Stabilized Zirconia Ceramics," J. Am. Ceram. Soc., 73 (1990), 893-903.
33. C. J. Gilbert, D. R. Dauskardt, R. W. Steinbrech, R. N. Petrany and R. O. Ritchie, "Cyclic Fatigue in Monolithic Alumina: Mechanisms for Crack Advanced Promoted by Fractional Wear of Grain Bridges," J. Mater. Sci., 30 (1995), 643-654.
34. C. J. Gilbert, R. H. Dauskardt and R. O. Ritchie, "Behavior of Cyclic Fatigue Cracks in Monolithic Silicon Nitride," J. Am. Ceram. Soc., 78 (1995), 2291-2300.
35. B. Lawn, Fracture of Brittle Solids, 2nd ed. (Cambridge University Press, New York, 1993).
36. S. Lathabai, J. Rödel, and B. Lawn, "Cyclic Fatigue from Frictional Degradation at Bridging Grains in Alumina," J. Am. Ceram. Soc., 74(1991), 1340-1348.
37. R. H. Dauskardt, "A Frictional-Wear Mechanism for Fatigue-Crack Growth in Grain Bridging Ceramics," Acta Metall. Mater., 41 (1993), 2765-2781.
38. P. L. Swanson, C. J. Fairbanks, B. R. Lawn, Y-W. Mai and B. J. Hockey, "Crack-Interface Grain Bridging as a Fracture Resistance Mechanism in Ceramics: I. Experimental Study on Alumina," J. Am. Ceram. Soc., 70 (1987), 279-289.
39. F. F. Lange, B. I. Davis, and M. G. Metcalf, J. Mater. Sci., "Strengthening of Polyphase Si<sub>3</sub>N<sub>4</sub> Materials Through Oxidation," 18 (1983), 1497-1505.
40. M. K. Cinibulk, G. Thomas, and S. M. Johnson, "Fabrication and Secondary-Phase Crystallization of Rare-Earth Disilicate-Silicon Nitride Ceramics," J. Am. Ceram. Soc., 75 (1992), 2037-2043.
41. M. K. Cinibulk, G. Thomas, and S. M. Johnson, "Oxidation Behavior of Rare-Earth Disilicate-Silicon Nitride Ceramics," J. Am. Ceram. Soc., 75 (1992), 2044-2049.
42. J. L. Ding, K. C. Liu, K. L. More, and C. R. Brinkman, "Creep and Creep Rupture of an Advanced Silicon Nitride Ceramic," J. Am. Ceram. Soc., 77 (1994), 867-874.
43. A. Rendtel and H. Hübner, "Silicon Nitride/Silicon Carbide Nanocomposite Materials: II, Hot Strength, Creep, and Oxidation Resistance," J. Am. Ceram. Soc., 81 (1998), 1109-1120.